ORIGINAL RESEARCH ARTICLE

Predictors and prognosis of right ventricular function in pulmonary hypertension due to heart failure with reduced ejection fraction

Alexander Schmeißer[1], Thomas Rauwolf[1]* (iD), Thomas Groscheck[1], Katharina Fischbach[2], Siegfried Kropf[3], Blerim Luani[1], Ivan Tanev[1], Michael Hansen[1], Saskia Meißler[1], Kerstin Schäfer[1], Paul Steendijk[4] and Ruediger C. Braun-Dullaeus[1]

[1]*Department of Internal Medicine, Division of Cardiology and Angiology, Magdeburg University, Leipziger Str. 44, Magdeburg, D-39120, Germany;* [2]*Department of Radiology, Magdeburg University, Magdeburg, Germany;* [3]*Institute of Biometry and Medical Informatics, Magdeburg University, Magdeburg, Germany;* and [4]*Department of Cardiology, Leiden University Medical Center, Leiden, The Netherlands*

Abstract

Aims Failure of right ventricular (RV) function worsens outcome in pulmonary hypertension (PH). The adaptation of RV contractility to afterload, the RV-pulmonary artery (PA) coupling, is defined by the ratio of RV end-systolic to PA elastances (Ees/Ea). Using pressure–volume loop (PV-L) technique we aimed to identify an Ees/Ea cut-off predictive for overall survival and to assess hemodynamic and morphologic conditions for adapted RV function in secondary PH due to heart failure with reduced ejection fraction (HFREF).

Methods and results This *post hoc* analysis is based on 112 patients of the prospective Magdeburger Resynchronization Responder Trial. All patients underwent right and left heart echocardiography and a baseline PV-L and RV catheter measurement. A subgroup of patients (n = 50) without a pre-implanted cardiac device underwent magnetic resonance imaging at baseline. The analysis revealed that 0.68 is an optimal Ees/Ea cut-off (area under the curve: 0.697, $P < 0.001$) predictive for overall survival (median follow up = 4.7 years, Ees/Ea ≥ 0.68 vs. <0.68, log-rank 8.9, $P = 0.003$). In patients with PH (n = 76, 68%) multivariate Cox regression demonstrated the independent prognostic value of RV-Ees/Ea in PH patients (hazard ratio 0.2, $P < 0.038$). Patients without PH (n = 36, 32%) and those with PH but RV-Ees/Ea ≥ 0.68 showed comparable RV-Ees/Ea ratios (0.88 vs. 0.9, $P = 0.39$), RV size/function, and survival. In contrast, secondary PH with RV-PA coupling ratio Ees/Ea < 0.68 corresponded extremely close to cut-off values that define RV dilatation/remodelling (RV end-diastolic volume >160 mL, RV-mass/volume-ratio ≤0.37 g/mL) and dysfunction (right ventricular ejection fraction <38%, tricuspid annular plane systolic excursion <16 mm, fractional area change <42%, and stroke-volume/end-systolic volume ratio <0.59) and is associated with a dramatically increased short and medium-term all-cause mortality. Independent predictors of prognostically unfavourable RV-PA coupling (Ees/Ea < 0.68) in secondary PH were a pre-existent dilated RV [end-diastolic volume >171 mL, odds ratio (OR) 0.96, $P = 0.021$], high pulsatile load (PA compliance <2.3 mL/mmHg, OR 8.6, $P = 0.003$), and advanced systolic left heart failure (left ventricular ejection fraction <30%, OR 1.23, $P = 0.028$).

Conclusions The RV-PA coupling ratio Ees/Ea predicts overall survival in PH due to HFREF and is mainly affected by pulsatile load, RV remodelling, and left ventricular dysfunction. Prognostically favourable coupling (RV-Ees/Ea ≥ 0.68) in PH was associated with preserved RV size/function and mid-term survival, comparable with HFREF without PH.

Introduction

The functional and hemodynamic sequelae of pulmonary hypertension (PH) are directly linked to the relationship between pulmonary vascular load and the adaptive intrinsic contractility response of the right ventricle (RV) coupled to the load [right ventricular-pulmonary arterial (RV-PA) coupling]. The gold standard to quantify RV-PA coupling *in vivo* is the conductance catheter technique, which acquires pressure and volume simultaneously on a beat-to-beat basis.[1] The pressure–volume (PV) loop-derived, load-independent index of RV contractility, the end-systolic elastance (Ees), put into relation to end-systolic arterial elastance (Ea), an accepted measure of global RV afterload, determines the coupling of intrinsic RV contractility to afterload (Ees/Ea: RV-PA coupling).[2] Theoretically and evaluated mostly within models of left ventricle (LV) to systemic arterial coupling, optimal mechanical coupling occurs when Ees/Ea is equal to 1; the optimal energy transfer from the RV to the pulmonary circulation occurs at Ees/Ea ratios of 1.5–2.[3,4] However, there is a broad Ees/Ea range between 0.5 and 2.0 in which stroke work is still optimal,[3] at least in the LV. Tello *et al*.[5] recently prospectively examined 42 patients with precapillary PH using the invasive RV PV-loop single-beat technique and identified an Ees/Ea cut-off of 0.805 associated with RV failure. Richter *et al*.[6] identified a multi beat-derived Ees/Ea cut-off of 0.7 that was associated with clinical worsening in 38 mostly PAH patients. Although there is considerable focus on RV failure in PAH, the former is also of significant prognostic importance in patients with systolic left heart failure [heart failure with reduced ejection fraction (HFREF)] and secondary PH (Group-2 Nizza classification).[7] Clinical outcomes after advanced therapies, including guideline-directed medical/device therapy and LV assist devices, continue to be adversely affected by secondary postcapillary PH and/or RV dysfunction.[8] However, the pathophysiology of RV failure in secondary PH due to HFREF seems to be more complex than in PAH because more factors than a pure afterload increase affects RV contractility adaptation in this situation. Pulmonary vascular remodelling processes, for example, with a transition from isolated postcapillary PH to combined postcapillary and precapillary PH[9] and accentuation of pulsatile load,[10] describe the specific afterload characteristics in these patients. In addition, the RV may also be involved in the cardiomyopathic processes or the contractile LV dysfunction compromises the systolic LV to RV myocardial crosstalk.[11]

Therefore, the aim of the present study was to assess the ability of invasive PV loop-derived Ees/Ea ratio to predict the overall survival in HFREF patients with secondary PH, identify the best Ees/Ea cut-off for discrimination of prognosis, and evaluate possible predictors for RV-PA coupling efficiency. In addition, the capacity of different non-invasive parameters to discriminate between adaptive coupling and uncoupling in secondary PH was assessed.

Methods

The Magdeburger cardiac resynchronization therapy (CRT) responder trial was a prospective monocentric study of patients with HF with an indication for CRT (New York Heart Association II and III), sinus rhythm, left bundle branch block and HFREF.[12] The study was approved by the Institutional Review Board. All patients gave written informed consent. The investigation conformed with the principles outlined in the Declaration of Helsinki (*Br Med J* 1964; ii, p. 177).

This *post hoc* analysis is based on 112 patients, each with a baseline RV-PV loop measurement. All patients underwent right and left heart echocardiography and the PV loop and Swan-Ganz catheter measurement. In a subgroup of patients (*n* = 50) without an implanted device, a magnetic resonance imaging (MRI) of the heart was carried out. In order to enable a comparable fluid status of the individual patient, these examinations were carried out always within 2–3 days after admission, nothing per oral between 9 am and 11 am. The CRT (Boston Scientific, Marlborough, USA) was implanted in a standard manner, according to the study protocol, after baseline examination in 110 patients. Two patients declined the CRT implantation after baseline examination but agreed to the clinical follow-up and data analysis outside the study protocol. The clinical follow-up was performed every 6 months.

Echocardiography

Echocardiographic analysis was performed by two independent specialists using Xcelera and QLAB 8.1 Software (Phillips, The Netherlands). Mitral regurgitation was quantified by the criteria of functional mitral valve regurgitation (MR).[13] The forward stroke volume (SV) was quantified by the velocity time integral method in the aortic outflow tract. The tricuspid annular plane systolic excursion (TAPSE) and fractional area change (FAC), including the systolic and end-diastolic area, were measured according to current guidelines.[14]

Cardiac magnetic resonance (MRI)

A subgroup of patients (*n* = 50) without a pre-implanted cardiac device underwent MRI using a 1.5-T cardiac magnetic resonance scanner (Philips Medical Systems, The Netherlands) at baseline. Briefly, steady-state free precession cine images were acquired in multiple short-axis and long-axis views (electrocardiogram triggering, breath-hold technique). The analysis of RV volumes was performed by determining the end-diastolic and end-systolic frames on short-axis cine views, and semiautomated thresholding was used to

delineate the endocardial borders. The systolic descent of the tricuspid valve plane was tracked on long-axis views to correctly identify the ventricular volume in the basal short-axis slice.

RV mass

The area of myocardium in the end-diastolic short-axis slice was calculated by manually tracing the epicardial and endocardial borders of the right ventricular free wall for calculation of RV mass, using MRI software (Circle cvi42 version 5.12, Calgary, Canada). Papillary muscles were included. The interventricular septum was taken to be part of the LV. This process was repeated for each short-axis slice. Reproducibility of the RV measurements was tested in 10 randomly selected patients.

According the study by Badagliacca *et al.*,[15] the median of RV mass/volume ratios (RV M/V) was calculated in patients with secondary PH (0.37) and was used to divide the study population into patients with more adaptive (RV M/V ratio >0.37) and maladaptive RV remodelling (≤0.37).

Left and right heart catheterization, RV-PV loop catheter

The left and right heart catheter measurements were carried out as described previously.[16] The forward cardiac output was calculated using the Fick method. Trans-pulmonary gradient, diastolic pressure gradient, and pulmonary vascular resistance (PVR) were calculated using standard formulas. PA compliance was determined as ratio between forward SV and pulmonary pulse pressure. Secondary PH Group 2 was defined by a PA mean ≥25 mmHg and a pulmonary capillary wedge pressure >15 mmHg at rest. Isolated postcapillary PH was differentiated from the combined precapillary and postcapillary PH (CpcPH) by PVR < vs. ≥ 3 wood units, according to the proposed haemodynamic definition of the 6th World Symposium on Pulmonary Hypertension.[17]

PV loop measurement

A 7F RV-PV catheter (CD Leycom, The Netherlands) was positioned via the internal jugular vein for PV loop analysis. The PV loop was obtained beat-to-beat in real time during steady state (Inca©, CD Leycom, The Netherlands). The RV haemodynamics and RV pulmonary coupling were analysed by the CircLab software (Leiden University, The Netherlands). The calibration of RV conductance data, the parallel conductance, and the determination of the slope factor was performed as previously described.[18] RV end-systolic elastance (Ees = Piso − Pes/SV) was determined by using the single-beat PV-loop method described by Brimioulle *et al.*.[19] Determination of Piso was modified

by the approach of Ten Brinke *et al.*.[20] To complete the end-systolic PV relationship, we determined the volume intercept of end-systolic PV relationship (V25) at an RV pressure of 25 mmHg.[20] The RV afterload was determined by effective arterial elastance [single-beat (SB)-Ea, calculated as RV end-systolic pressure/SV]. Regarding the RV end-systolic point, we used the maximal RV pressure at minimum volume, which denotes the point of end-ejection, but not below RV dp/dt_{min} in the case of true triangular PV loop curves without a demarked shoulder region. Ventricular pulmonary coupling was quantified as SB-Ees/Ea (Supporting information *Figure S1*). For description of diastolic function of the RV, we calculated Tau and the SB-end-diastolic elastance (Eed) as previously described.[21]

A PV loop area was calculated as the sum of the potential energy and stroke work, and the mechanical efficiency as the quotient stroke work/PV loop area.[19,22]

Statistics

All data and statistics are reported as median and interquartile range [25–75%]. Categorical data were summarized by percentages. Baseline characteristics were compared using the Mann–Whitney *U* test. The receiver operating characteristic (ROC) analysis was used to derive a precise cut-off of Ees/Ea that would best discriminate all-cause mortality in PH patients. The Kaplan–Meier method was used to compare the different strata for estimation of the proportion of patients experiencing the endpoint of all-cause mortality compared with the log-rank test. Cox regression analysis was used for the analyses of independent predictors of mortality. Variables perceived as clinically important and those with a $P < 0.1$ in univariate analyses were included in the multivariate model. Differences with $P < 0.05$ were considered statistically significant. The multicollinearity was assessed. Parameters representing RV remodelling, LV-RV interaction and RV afterload were included in a univariate logistic binary regression analysis to determine the baseline factors predictive for prognostically relevant RV-PA coupling (cut-off of 0.68 for Ees/Ea found in ROC analysis). Parameters significant in the univariate analysis were added to a multivariate model. Multicollinearity was assessed. ROC analysis was used to identify cut-off values for potential predictors discriminating Ees/Ea ≥ 0.68 vs. <0.68. We analysed the relationship of non-invasive parameters of RV function and size with the haemodynamic PV loop-derived coupling ratio Ees/Ea and intrinsic RV contractility (Ees) *per se* using linear regression and ROC analyses and estimated cut-offs of non-invasive surrogates to discriminate the PV loop-derived Ees/Ea ≥ 0.68 vs. <0.68. The Statistical Package for Social Sciences software (SPSS 24, IBM, USA) was used.

Results

A total of 76 out of 112 (68%) patients with HFREF presented with secondary PH (PA mean ≥25 mmHg). The PV loop SB-derived RV-PA coupling ratio in these patients was 0.59 [0.42–0.89], determined by a RV intrinsic contractility Ees of 0.35 mmHg/mL [0.26–0.48] and a total afterload Ea of 0.57 mmHg/mL [0.44–0.81]. In patients without PH (n = 36, 32%) the Ees/Ea was 0.88 [0.7–1.1], calculated from an Ees of 0.25 mmHg/mL [0.2–0.32] and an Ea of 0.32 mmHg/mL [0.23–0.39], (Table 1).

Survival analysis

Thirty-six (47.4%) of the patients with secondary PH and seven (19%) without PH died during the median follow-up of 4.7 years [2.4–6.7] (χ^2 log-rank: 7.27; P = 0.007; Figure 1A). We used the ROC (supporting information) and Kaplan–Meier analysis (Figure 1B) to evaluate whether the PV loop-derived Ees/Ea may further discriminate overall survival from all-cause mortality in secondary PH. The area under the receiver operating curve (AUC) for Ees/Ea was 0.697, P < 0.001. We identified a cut-off of 0.68 for Ees/Ea

Table 1 Baseline characteristics

	No-PH (N = 36]	PH (PAP$_{mean}$ ≥ 25 mmHg) Ees/Ea ≥ 0.68 (N = 32]	PH (PAP$_{mean}$ ≥ 25 mmHg) Ees/Ea < 0.68 (N = 44]	P No-PH vs. Ees/Ea ≥ 0.68	P Ees/Ea < 0.68 vs. ≥ 0.68
Age (years)	63 (56–71]	65 (62–73]	71 (64–76]	0.27	0.06
Men [%]	86	84	84	0.84	0.94
ICM [%]	36	56	67	0.1	0.32
Beta-blocker (%)	100	96.9	95.3	0.29	0.74
ACE-I/AT blocker (%)	97.2	96.9	90.7	0.93	0.29
MRA (%)	66.7	50	42	0.166	0.29
CpcPH [%]	0	22	50	na.	0.014
Ea [mmHg/mL]	0.32 [0.23–0.39]	0.44 [0.34–0.53]	0.79 [0.55–0.99]	<0.001	<0.001
Ees [mmHg/mL]	0.25 [0.2–0.32]	0.43 [0.30–0.51]	0.3 [0.23–0.44]	<0.001	0.001
Ees/Ea	0.88 [0.7–1.1]	0.90 [0.8–1.1]	0.47 [0.31–0.56]	0.39	<0.001
ESV 25 [mL]	91 [73–110]	69 [53–91]	50 [38–72]	0.002	0.011
PVA [mL * mmHg]	2,862 [2,223–3,681]	3,802 [3,057–5,211]	6,658 [5,601–8,886]	<0.001	<0.001
Mechanical efficiency	0.69 [0.57–0.76]	0.67 [0.62–0.72]	0.43 [0.34–0.51]	0.98	<0.001
SV/ESV (MRI)	0.97 [0.78–1.1]	0.89 [0.77–1.1]	0.39 [0.25–0.48]	0.8	<0.001.
Tau [ms]	63 [56–75]	63 [55–70]	71 [60–83]	0.84	0.013
RVEDP [mmHg]	6.8 [5–9.4]	7.4 [6–11.6]	10.7 [8.1–13.6]	0.165	0.008
Eed [mmHg/mL]	0.056 [0.04–0.07]	0.068 [0.05–0.085]	0.077 [0.06–0.12]	0.049	0.041
PASP [mmHg]	30 [28–33	41 [38–53]	60 [52–74]	<0.001	<0.001
PA mean [mmHg]	20 [18–22]	28 [26–35]	41 [34–46]	<0.001	<0.001
PA compliance [mL/mmHg]	4.3 [3.3–4.8]	2.7 [2.2–3.5]	1.5 [1.2–2.1]	<0.001	<0.001
PVR [dyn.]	135 [93–191]	181 [121–215]	252 [197–375]	0.07	0.001
diastolic TV annulus diameter [mm]	37 [33–45]	37 [33–42]	50 [46–55]	0.68	<0.001
RVEDV [PV loop] [mL]	153 [138–169]	165 [150–179]	193 [172–227]	0.08	<0.001
RVEDV [MRI] [mL]	134 [119–161]	127 [108–141]	209 [169–247]	0.27	<0.001
RVESV [MRI] [mL]	71 [57–88]	66 [53–79]	155 [112–181]	0.65	<0.001
RVEF [MRI] [%]	51 [45–54]	50 [47–55]	28 [21–33]	0.84	<0.001
RV mass (MRI, g)	51.4 [44–61]	50 [45–57]	63 [56–71]	0.91	0.008
RVmass/BSA (MRI, g/m^2)	25.9 [23.6–29]	25.8 [24.4–27.3]	29.6 [27.6–32.9]	0.77	0.012
RV M/V ratio (MRI, g/mL)	0.39 [0.33–0.41]	0.41 [0.36–0.47]	0.28 [0.27–0.32]	0.14	0.001
RV M/V ratio cut-off > 0.37 g/mL (%)	62.5	71.4	9.1	0.61	0.002
FAC [%]	53 [45–59]	54 [49–57]	31 [26–35]	0.53	<0.001
TAPSE [mm]	19 [16–23]	20 [18–22]	13 [10–15]	0.47	<0.001
TAPSE/PASP [mm/mmHg]	0.6 [0.5–0.8]	0.5 [0.35–0.54]	0.2 [0.15–0.30]	<0.001	<0.001
TR 2/3 [%]	0	9.7	38.7	0.94	<0.001
MR 2/3 [%]	11.4	16.1	50	0.37	0.004
LV-EF [%]	35 [30–37]	33 [30–35]	27 [24–33]	0.88	<0.001
LVEDV [mL]	214 [175–261]	200 [175–239]	217 [189–287]	0.58	0.11
LA volume [mL]	66 [51–110]	79 [60–96]	99 [85–124]	0.5	0.001

4chv, 4 chamber view; ACE-I, angiotensin converting enzyme inhibitor; AT, angiotension receptor; CpcPH, combined precapillary and postcapillary PH; Ea, pulmonary arterial elastance; Eed, RV end-diastolic elastance; Ees, right ventricular end-systolic elastance; ESV, end-systolic volume; ESV$_{25}$, right ventricular volume at pressure 25 mmHg; FAC, RV fractional area change; ICM, ischemic cardiomyopathy; M, mass; MRA, mineralocorticoid receptor antagonist; PA-Ca, pulmonary arterial compliance; PA$_{mean}$, mean pulmonary arterial pressure; PAP$_{mean}$, mean pulmonary arterial pressure; PASP, systolic pulmonary arterial pressure; PH, pulmonary hypertension; PV, pressure–volume; PVR, pulmonary vascular resistance; RVEDV, right ventricular end-diastolic volume; RVEF, right ventricular ejection fraction; SV, stroke volume; TAPSE, tricuspid annular plane systolic excursion; Tau, time constant for isovolumic relaxation; TV, tricuspid valve; V, volume.
Values are median [25th/75th percentiles].

Figure 1 Survival analysis. (A) Kaplan–Meier estimates of time to all-cause death stratified by pulmonary hypertension (PH) vs. no-PH in patients with heart failure with reduced ejection fraction (HFREF) [PH is defined by pulmonary artery (PA) mean ≥25 mmHg]. (B) Kaplan–Meier estimates of time to death stratified by HFREF patients without PH (no-PH) and PH patients stratified by the pressure–volume (PV) loop-derived Ees/Ea ratio (≥0.68 vs. <0.68). (C) Boxplot analysis of the PV loop-derived Ees/Ea of HFREF patients without PH (No-PH) and PH patients stratified according to the Ees/Ea ratio cut-off of 0.68. PH: (PA mean ≥25 mmHg), No-PH: HFREF patients with PA mean <25 mmHg. AUC, area under the curve; Ees, RV end-systolic elastance; Eea, pulmonary arterial end-systolic elastance.
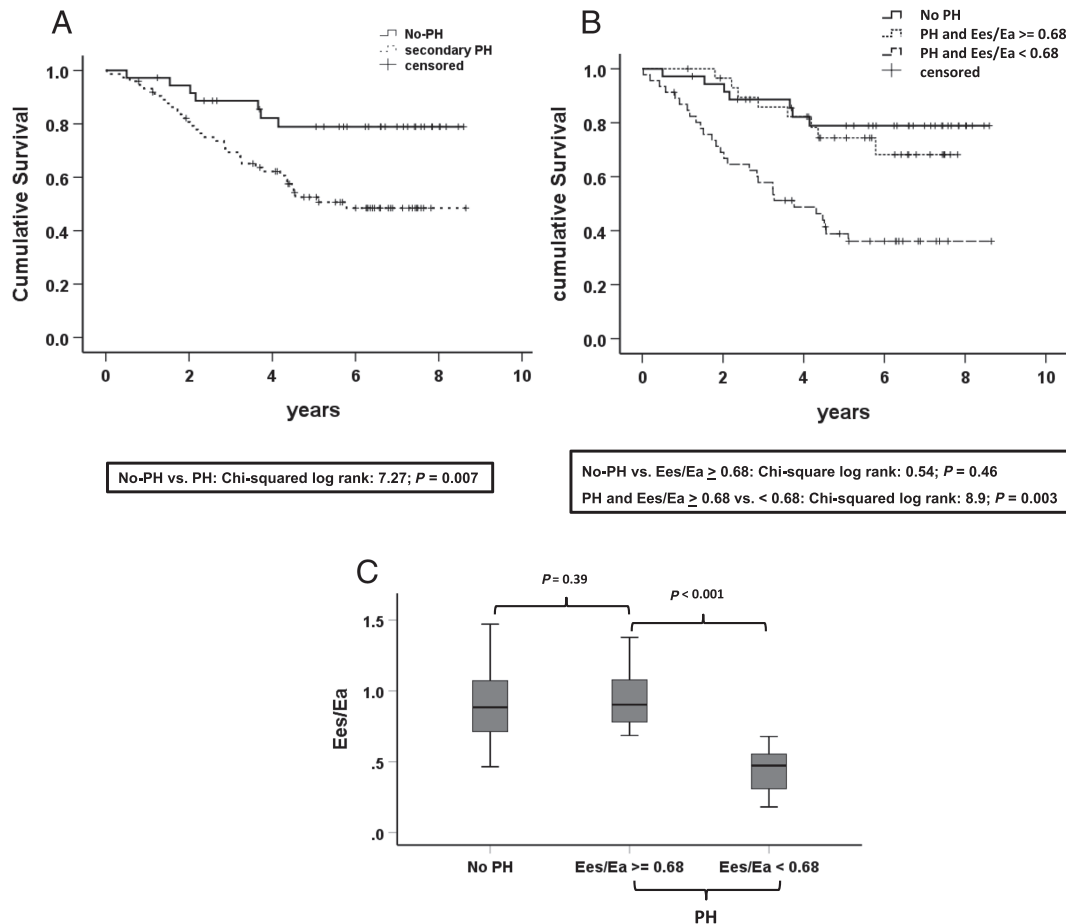
with a sensitivity of 74% and a specificity of 61% for discrimination of medium-term survival from all-cause mortality. Kaplan–Meier analysis revealed that patients with PH and PV loop-derived Ees/Ea ≥ 0.68 had a significantly better prognosis than those with a lower Ees/Ea ratio (χ^2 log-rank: 8.9, P = 0.003) (*Figure 1B*). Multivariate Cox regression analysis could demonstrate the independent predictive value of the PV loop-derived Ees/Ea for prognosis in patients with secondary PH with a hazard ratio of 0.2 (P = 0.038, *Table 2*). Conversely, we found comparable Ees/Ea ratios between HFREF patients without PH (No-PH) and those with PH and favourable coupling (Es/Ea ≥ 0.68), 0. 88 [0.7–1.1] vs. 0.9 [0.8–1.1], P = 0.39, respectively, which was accompanied by a statistically not different median survival time between these two groups (χ^2 log-rank: 0.54, P = 0.46) (*Figures 1B* and *2*). Determination of the Ees/Ea cut-off and the analysis of associated survival within the subgroup of patients with

a baseline MRI were shown within figures: supplement MRI subgroup.

Representative PV loops of the three groups studied are demonstrated in the supporting information.

Comparison of haemodynamics and RV function of PH patients stratified by the Ees/Ea cut-off of 0.68

Comparing both PH groups, stratified by the Ees/Ea ratio of 0.68, we found that patients with Ees/Ea < 0.68 were characterized by significantly lower intrinsic RV contractility (Ees) and higher medians of the different afterload parameter (total RV afterload Ea, pulsatile load: PA compliance, and steady state load: PVR) than patients with Ees/Ea ≥ 0.68. These findings were associated with more dilated [RV

Table 2 Multivariate Cox regression with baseline data to predict all-cause mortality in patients with PH (PA pressure mean ≥25 mmHg)

Variables	Multivariate		
	HR	(95% CI)	P value
Ees/Ea	0.151	(0.037–0.619)	0.003
PA compliance	0.518	(0.335–0.799)	0.003

CI, confidence interval; DPD, diastolic pressure gradient; Ea, effective arterial elastance; Eed, end-diastolic elastance; Ees, end-systolic elastance; EF, ejection fraction; HR, hazard ratio; LVESDV, left ventricular end-diastolic volume; LVESV, left ventricular end-systolic volume; MR, mitral valve regurgitation; PA, pulmonary artery; PCWP, pulmonary capillary wedge pressure. Additional baseline univariate variables associated with all-cause mortality ($P < 0.1$) entered the multivariate model: PVR, PA compliance, PCWP, mitral regurgitation (Degree 0-III), tricuspid regurgitation; Eed; Ea and existence of CpcPH. (as categorical and/or continuous variable).
Age, LVEF, Ees, RC time, DPD, Tau, LVEDV, and LVESV did not enter the model because univariate analysis showed $P > 0.1$.

end-diastolic volume (RVEDV)] and remodelled (RV mass/volume ratio) RVs, worse systolic (RV-EF, TAPSE, and FAC) and diastolic (Tau and Eed) function, and a higher proportion of significant tricuspid regurgitation in the Ees/Ea < 0.68 group. In addition, this prognostically unfavourable group was associated with a significant lower left ventricular function (LV-EF) and a higher proportion of patients with significant MR 2/3 (*Table 1*, *Figure 2*).

Comparison of prognostically favourably coupled PH patients (Ees/Ea ≥ 0.68) with HFREF patients without PH

The higher total afterload Ea in PH patients with a Ees/Ea ≥ 0.68 resulted in an adaptive RV contractility (Ees) increase (*Figure 2*) and coupling ratios of Ees/Ea in the same range as in No-PH patients (*Table 1*, *Figure 1*). This was associated with comparable, nearly normal sized RVs with a preserved systolic function and RV relaxation (Tau), in contrast to a slightly, but significantly higher end-diastolic elastance (Eed) (*Table 1*, *Figure 2*) and comparable parameter of left heart function (*Table 1*).

Predictors of prognostically favourable vs. unfavourable RV-PA coupling (Ees/Ea cut-off of 0.68) in secondary PH

Scatter plot analysis of the relationship of Ees to Ea (*Figure 3A*) shows that non-adaptive RV contractility (Ees) regulation increases with increasing afterloads (Ea). Prognostically favourable coupling could no longer be practically observed above an Ea of ~ 0.8 mmHg/mL. However, non-adaptive RV contractility regulation may also exist at only slightly to moderately increased Ea values. This is indicated by a flatter

increase of the regression line between Ees and Ea in the unfavourably coupled group (Ees:Ea r = 0.59, $P < 0.001$, $y = 0.27 * x + 0.12$) compared with the favourably coupled group (Ees/Ea: r = 0.8, $P < 0.001$, $y = 0.7 * x + 0.11$) (*Figure 3A*). Independent determinants of prognostically favourable contractility adaptation to afterload in the multivariate logistic bivariate regression analysis were higher PA compliances (OR 8.6), higher LV-EFs (OR 1.23) and a smaller RVEDV (OR 0.96) (*Table 3*, *Figure 3B–D*). We identified cut-offs of 2.3 mL/mmHg for PA compliance, 171 mL for RVEDV and 30% for LV-EF using ROC analysis to discriminate the RV-PA coupling ≥0.68 vs. <0.68 (*Figures S3* and *3B–D*). Correlation analyses between predictors of uncoupling and PV-loop and Swan-Ganz parameter are demonstrated (*Table S1* and *Figures S5* and *S6*).

The capacity of non-invasive parameters to discriminate between prognostically favourable and unfavourable RV-PA coupling in secondary PH

In ROC analysis we identified MRI cut-offs of 38% for RV-EF and 0.59 for SV/ESV ratio. Echocardiographic cut-offs were 16 mm for TAPSE and 42% for FAC with sensitivities and specificities above 90% and 85%, respectively, to discriminate a prognostically favourable and unfavourable RV-PA coupling, dichotomized at an Ees/Ea cut-off of 0.68 (*Table 4*). Linear regression analysis of the association of PV-loop-derived Ees/Ea, and Ees with non-invasive RV function/size in PH patients is demonstrated in *Tables S2* and *S3* and *Figure 4* and in patients without PH in *Table S4*.

Discussion

The results of our study demonstrate that the haemodynamic coupling of RV contractility (Ees) to increased afterload (Ea) determines RV size and function and is of independent prognostic value in patients with HFREF and secondary PH. The best cut-off for PV loop-derived SB Ees/Ea to discriminate overall survival was 0.68. The corresponding cut-offs for the non-invasively determined echo parameter right ventricular ejection fraction (RVEF) (38%), TAPSE (16 mm), FAC (42%), and MRI parameter RVEDV (160 mL) are very close to known prognostic cut-offs for RV dysfunction characterized by a decrease of RV-EF[7] below the critical value of 35%, TAPSE below 16 mm,[23] and FAC below 40%.[24] Our data also lead to the conclusion that the coupling of RV contractility to afterload has a considerable reserve in PH secondary to HFREF, as Ees/Ea has to decrease from theoretical functional optimal values of ≥1 to <0.68 before substantial RV maladaptation occurs and overall survival worsens. However, our cut-off of

Figure 2 Box plot analysis of haemodynamically and non-invasively evaluated RV function and morphology according the stratified patient groups (no-PH, PH and Ees/Ea ≥ vs. <0.68). (A) Pressure–volume (PV) loop-derived intrinsic RV contractility Ees vs. afterload Ea: Showing an adaptive Ees increase to increased EA in PH-Ees/Ea ≥ 0.68 with the resulting similar Ees/Ea values between no-PH and PH with an Ees/Ea ratio ≥0.68. A significantly higher afterload of Ea in PH-Ees/Ea < 0.68 compared to PH-Ees/Ea ≥ 0.68 (*P* < 0.001) could be observed, accompanied by a non-adaptive significantly lower Ees (*P* = 0.001). (B) MRI-derived RV end-systolic and -diastolic volumes, (C,D) RV mass/BSA and RV mass/volume ratio. (E,F) MRI-derived RV-ejection fraction (RV-EF) in the subgroup of patients without an implanted device and TAPSE in all patients with heart failure with reduced ejection fraction (HFREF). (G,H) PV-loop derived Tau and Eed. Eed, end-diastolic elastance; Ees, right ventricular end-systolic elastance; Ea, pulmonary arterial end-systolic elastance; MRI, magnetic resonance imaging; PH, pulmonary hypertension (PA mean ≥25 mmHg); no-PH, HFREF patients without PH; RVESV, right ventricular end-systolic volume; RVEDV, right ventricular end-diastolic volume; RV-EF, RV ejection fraction; TAPSE, tricuspid annular plane systolic excursion; Tau, relaxation time constant.
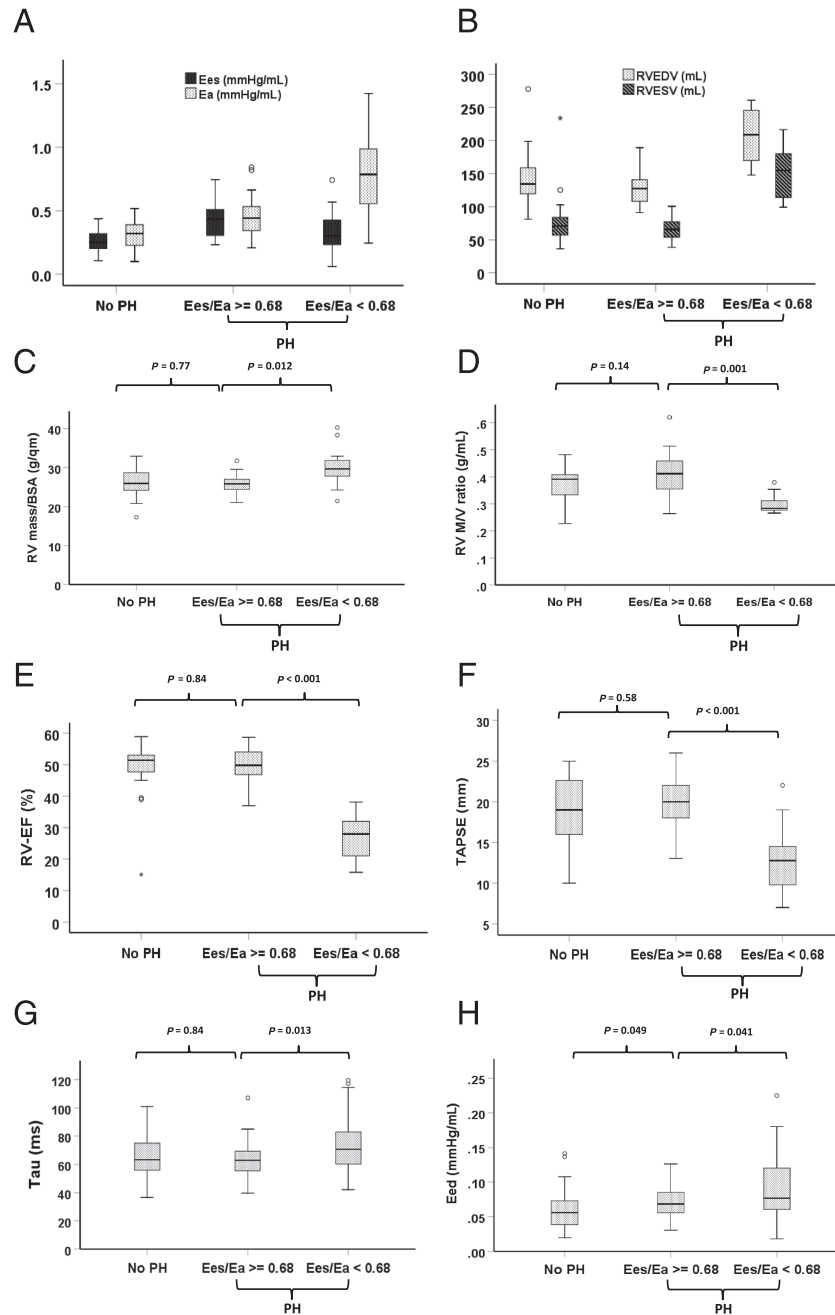
Figure 3 Relationship of intrinsic RV contractility of Ees to afterload Ea in patients with PH. A: Stratified by the prognostically relevant cut-off of 0.68 for pressure–volume (PV) loop-derived Ees/Ea. The straight lines denote the regression lines for both differently coupled groups. Patients with a PH-Ees/Ea ≥ 0.68 demonstrated the tighter correlation between Es and Ea and a steeper regression line than PH patients with an Ees/Ea < 0.68. (B) PA compliance is an independent predictor of prognostically relevant RV-PA coupling dichotomized at an Ees/Ea of 0.68. The straight line denotes an Ees/Ea ratio of 0.68. The best cut-off of PA compliance to discriminate an Ees/Ea of 0.68, determined by receiver operating characteristic (ROC) analysis, was 2.3 mL/mmHg. Patients with a PA compliance ≥2.3 mL/mmHg were marked by an asterisk (*). Hollow circles denote patients with PA compliance <2.3 mL/mmHg. Right: Box plot analysis of the median PA compliance in PH patients according to the Ees/Ea ratio ≥ vs. < 0.68. (C) RVEDV is an independent predictor of prognostically relevant RV-PA coupling dichotomized at an Ees/Ea of 0.68. The straight line denotes an Ees/Ea ratio of 0.68. The best cut-off of RVEDV to discriminate an Ees/Ea of 0.68, determined by ROC analysis, was 171 mL. Patients with a RVEDV <171 mL were marked with an asterisk (*) and are more concentrated left of the regression line of Ees/Ea = 0.68. Hollow circles denote patients with RVEDV ≥171 mL. Right: Box plot analysis of the median RVEDV in PH patients according the Ees/Ea ratio ≥ vs. < 0.68. (D) LV-EF is an independent predictor of prognostically relevant RV-PA coupling dichotomized at an Ees/Ea of 0.68. The straight line denotes an Ees/Ea ratio of 0.68. The best cut-off of LV-EF to discriminate an Ees/Ea of 0.68, determined by ROC analysis, was 30%. Patients with an EF ≥ 30% were marked with an asterisk (*) and are more concentrated left of the regression line of Ees/Ea = 0.68. Hollow circles denote patients with LV-EF < 30%. Right: Box plot analysis of the median LV-EF in PH patients according the Ees/Ea ratio ≥0.68 vs. <0.68. Eea, pulmonary arterial end-systolic elastance; Ees, RV end-systolic elastance; LV, left ventricle; EF, ejection fraction; PH, pulmonary hypertension; PA, pulmonary artery; RV, right ventricle; RVEDV, RV end-diastolic volume.
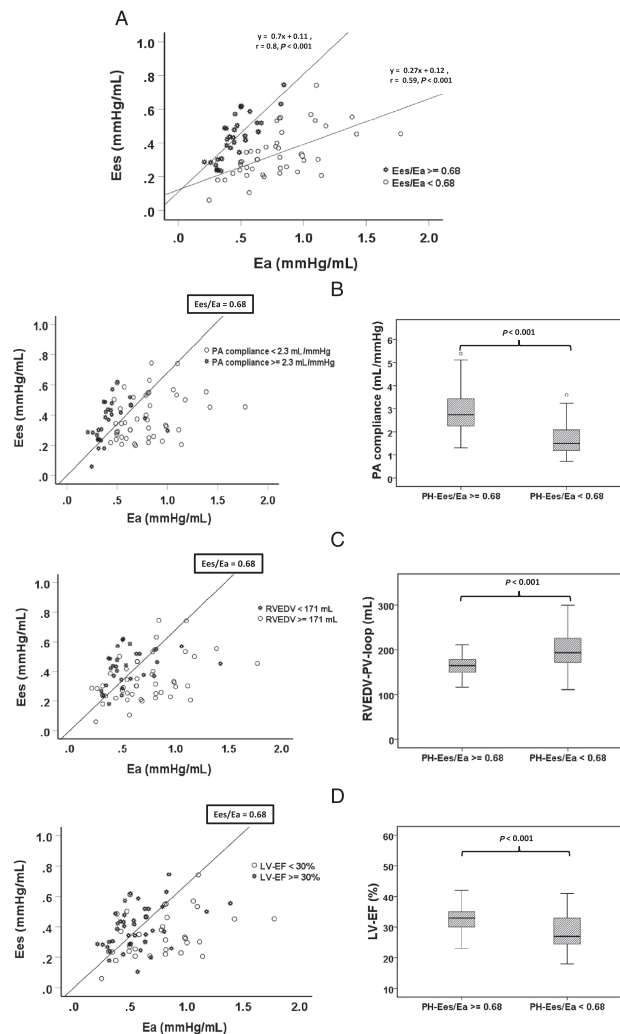
0.68 in postcapillary PH was lower than the SB-derived cut-off of 0.8 found in precapillary PAH/CTEPH patients[5] to detect pending RV failure (RV-EF < 35%), but closer to the multi-beat-derived cut-offs of 0.7[6,25] or 0.65[26] predicting clinical worsening in PAH/CTEPH patients. Different patient groups with different PH pathologies (precapillary vs. postcapillary) and different PV loop analysis methods (different SB methods[5] or using the multi-beat analysis[6,25,26]) may explain this distinction. In addition, it must be noted that the statistical power of the Ees/Ea cut-off of 0.68 to discriminate

Table 3 Multivariate binary logistic analysis for determinants of prognostically favourable RV-PA coupling (Ees/Ea > 0.68) in secondary PH

Variables	Odds ratio	95% CI	P value
PA compliance	8.6	2.1–35.3	0.003
LV-EF	1.23	1.023–1.482	0.028
RVEDV (PV loop)	0.96	0.926–0.994	0.021

CI, confidence interval; CpcPH, combined postcapillary and precapillary PH; IpcPH, isolated postcapillary pulmonary hypertension; LV-EF, left ventricular ejection fraction; LVESP, LV end-systolic volume; PA, pulmonary arterial; PV, pressure–volume; PVR, pulmonary vascular resistance; RVEDV, right ventricular end-diastolic volume.
Additional baseline univariate variables associated with favourable RV-PA coupling ratio ≥0.68 (P < 0.1) entered the multivariate binary logistic regression model: Left atrial volume, PVR, existence of CpcPH vs. IpcPH, PA mean, LVESP, mitral regurgitation, tricuspid regurgitation, arterial pulse pressure.
RC time, DPD, ischemic vs. dilative cardiomyopathy, and LVEDV did not enter the model because univariate analysis showed P > 0.1.
The main components of RV afterload, the steady state load (PVR) and the pulsatile load (PA compliance) were used for analysis of the global afterload measuring parameter Ea.

medium-term all-cause mortality (AUC 0.697, P = 0.005) is only moderate with a sensitivity and specificity of 74% and 61%, respectively. This appears slightly lower than the PV-loop-derived cut-off data collected in patients with PAH/CTEPH (Hsu *et al*.[26]: n = 26, AUC 0.78, Richter *et al*.,[6] N = 38, AUC 0.736). However, Hsu *et al*. discriminated their patients only regarding clinical worsening, which may be a softer clinical endpoint than all-cause mortality. In addition, our cohort of HFREF patients with secondary PH was older and had multiple reasons to die in medium term. Nevertheless, after testing of different left ventricular and RV-pulmonary vascular parameters, the multivariate Cox regression could show that the Ees/Ea ratio remained independently predictive for survival.

We looked for determinants of prognostically favourable vs. unfavourable RV-PA coupling in HFREF and secondary PH, as well. The logistic bivariate regression analysis revealed that the height of pulsatile afterload (PA compliance), the degree of RV remodelling (RVEDV, measured by PV loops) and the extent of LV dysfunction (LV-EF) with cut-offs of 2.3 mL/mmHg, 171 mL, and 30%, respectively, were parameters that independently predicted the RV-PA coupling ratio, dichotomized at 0.68. Prior, date from mostly experimental precapillary PH models (with normal LV function) had demonstrate that a progressive increase in afterload, above borders that are not yet clearly defined, may change the primarily adapted homeometric contractility regulation to increasingly heterometric response.[27] In fact, a prognostically favourable coupling was hardly found above an Ea of ~0.8 mmHg/mL. Interestingly, our data imply that the height of pulsatile load (lower PA compliance), even at only slightly to moderately increased total afterloads (Ea), independently affected the RV-PA coupling capacity. Several studies in left heart failure have shown that an elevated left atrial pressure reduces PA compliance out of proportion to PVR, thereby increasing RV pulsatile loading and worsening prognosis.[10,28] Additionally, a compromised RV due to an additional intrinsic involvement for example in left or right heart disease (such as myocarditis and RV infarction) cloud further increase RV (pulsatile) afterload sensitivity.[29,30] Furthermore, earlier experimental studies appreciated the significant contribution of LV contraction itself to RV systolic performance. [11] In fact, we could demonstrate that an advanced LV dysfunction (LV-EF < 30%) was independently associated with an unfavourable RV Ees/Ea ratio. Unfortunately, our study does not differentiate between RV remodelling because of long-standing PH-associated heterometric maladaptation and/or RV injury by involvement in the LV disease process.

Table 4 Receiver operating characteristic analysis of non-invasive imaging parameter to discriminate haemodynamic PV loop-derived favourable from unfavourable RV-PA coupling, stratified by Ees/Ea ≤ 0.68 vs. Ees/Ea > 0.68

	AUC	P	Cut-off	Sensitivity	Specificity
MRI					
MRI-RVEF (%)	0.99	<0.001	38	94	93
MRI-RVESV (mL)	0.99	<0.001	100	91	93
MRI-RVEDV (mL)	0.96	<0.001	160	94	86
MRI-SV/ESV	0.99	<0.001	0.59	93	94
Echo					
FAC (%)	0.98	<0.001	42	97	88
TAPSE (mm)	0.94	<0.001	16	90	86
ES area 4chv (cm^2)	0.93	<0.001	13	87	86
TAPSE/PASP (mm/mmHg)	0.91	<0.001	0.34	81	86
SV/ESV (PV-loop)	0.86	<0.001	0.69	80	78
ED 4chv area (cm^2)	0.81	<0.001	22	70	81
PASP (mmHg)	0.81	<0.001	52	75	67
LVEF (%)	0.72	<0.001	30	64	77

AUC, area under the curve; ED 4chv, echocardiographic 4-chamber view; ED, end-diastolic; EF, ejection fraction; ES, end-systolic; ESV, end-systolic volume; FAC, fractional area shortening (echo); MRI, magnetic resonance imaging; PASP, pulmonary arterial systolic pressure; PV, pressure–volume; RV, right ventricle; RVEDV, RV end-diastolic volume; RVEF, right ventricular ejection fraction; RVESV, RV end-systolic volume; SV, total stroke volume; TAPSE, tricuspid annular plane systolic excursion.

Figure 4 Linear regression analysis of the relationship between the pressure–volume (PV) loop-derived Ees/Ea ratio and RV size/function, and the SV/ESV ratio as potential non-invasive surrogates for haemodynamic coupling ratio Ees/Ea. The magnetic resonance imaging analysis within the subgroup of patients without an implanted device. Eea, pulmonary arterial end-systolic elastance; Ees, RV end-systolic elastance; RVEDV, RV end-diastolic volume; RVESV, RV end-systolic volume; RV-EF, RV-ejection fraction; SV, stroke volume.
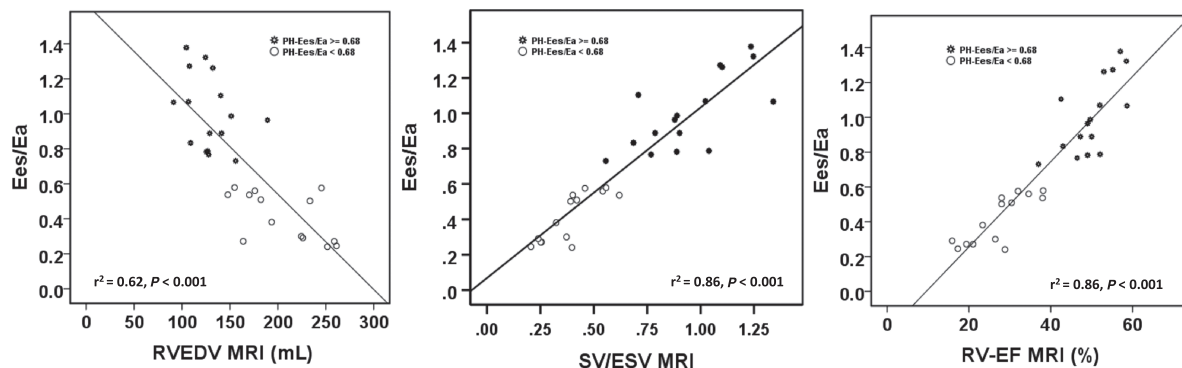
How might our comprehensive and complex haemodynamic data translate into meaningful clinical impact?

HFREF is a progressive disease with high morbidity and reduced prognosis, despite modern drug and device therapy. The development of secondary PH in these patients is frequent and has an important additional impact on disease progression, morbidity, and mortality, and warrants a particular close clinical attention.[9] A very interesting finding in our *post hoc* analysis is that patients with secondary PH and an RV-PA coupling ratio ≥0.68 have an overall survival that, at least in the medium term, is as good as HFREF patients without PH. Despite different afterloads, the comparable survival was associated with comparable RV-PA coupling ratios and consecutively near-normal RV sizes, systolic function, and relaxation (Tau) in both groups. Only, the end-diastolic elastance (Eed), as surrogate for diastolic RV stiffness, was significantly worse in prognostically favourably coupled patients. These data imply that RV contractility response to PH is closely associated to preserved RV systolic function/size and can cover up the prognostic influence of PH, at least in the medium term. These findings confirm the landmark data from Ghio *et al.*,[31] showing that secondary PH increases mortality in HFREF patients only in association with systolic RV dysfunction. In consequence, in HFREF patients with normal sized and functional RV in echocardiography, a prognostically favourable RV coupling can be assumed, independently of the existence of secondary PH. A comprehensive invasive catheter investigation of an existing secondary PH does not provide any additional benefit for risk stratification in this specific situation. In contrast, a PV-loop-derived Ees/Ea ratio <0.68 corresponded extremely close to cut-off values that define RV remodelling (RVEDV > 160 mL) and dysfunction (RVEF < 38%, TAPSE < 16 mm, FAC < 42%, *Table 4*) and

was associated with a dramatically increased short-term and medium-term all-cause mortality. Especially, patients with LV-EF < 30% and high pulsatile load (low PA compliance, closely associated with high LA/pulmonary capillary wedge pressure filling pressures, and the existence of moderate to severe MR) seem at significantly increased risk for a progressive RV-PA uncoupling (*Figure S6*). Echocardiographic evidence of a remodelled and/or dysfunctional RV in HFREF with secondary PH almost certainly indicates a prognostic unfavourable RV-PA coupling, which warrants particular attention regarding the adjustment of drug and device therapy (including interventional reduction of severe MR) but also for planning of heart transplantation and/or implantation of left ventricular assist devices (LVADs). An invasive haemodynamic investigation of the RV-PA-left atrial axis with the Swan-Ganz catheter technique, including testing pulmonary vasoreactivity, appears absolutely necessary in this situation. Nevertheless, acute right heart failure (RHF) remains a frequent complication after LVAD implantation,[32] yet the definition of RHF and preimplant variables that predict RHF remain controversial. The PV-loop-derived analysis of RV intrinsic contractility response to afterload could be a promising method to improve the preimplant risk stratification in these patients. In this setting, the modulation of RV afterload with PDE-5-inhibitors (PDE5i) in order to improve RV function prior to LVAD implantation for prevention of early RHF is still a matter of debate. Several small clinical studies with positive effects of PDE5i on RV function and outcomes in HFREF patients after LVAD/heart transplantation[33] are contradicted by a recent analysis of the INTERMACS database,[34] which suggested that patients routinely preoperatively treated with PDE5i had higher rates of post LVAD-RV failure. A blunted inotropic response to beta-agonists induced by PDE5i,[35] and/or a pulmonary-left ventricular overflow due to loss of any ostensible protective precapillary pulmonary

vasoconstriction are discussed.[36] Very recent promising findings challenge this concept.[37] Monzo et al.[37] could show that acute PDE5i administration did not change contractility but had profound afterload reducing effects, improved RVEF and RV volumes and lowered LA filling pressure through relief of pericardial constraint in patients with advanced HFREF and secondary PH. Despite comparable LA filling pressures between both study groups (23.9 vs. 25.1 mmHg, Monzo et al.[37] vs. INTERMACS[34]), the patient cohort in the study by Monzo et al. [37] was characterized by a pronounced 'out-of-proportional' increase of TPG (17.6 vs. 10 mmHg) and PVR (PVR 4.9 vs. 2.6 WU), which defines their patients as mostly combined precapillary and postcapillary PH patients in comparison with INTERMACS patients with mostly isolated postcapillary PH. In fact, the afterload reducing effects of acute PDE5i administration in these combined precapillary and postcapillary PH patients was relatively selective in lowering the 'out-of-proportional' increased TPG and PVR. However, more data are needed for definition of a probable subgroup of HFREF patients where PDE5i prior to LVAD implantation have beneficial effects. Especially, the intensely debated role of PDE5i for modulation of right ventricular contractility in HFREF with secondary PH and remodelled RV needs more clarification with better methods. Using the RV PV-loop technique in this setting, new and better insights in this field are expected.

Our study has several limitations. This is a *post hoc* analysis of a single-centre, prospective observational study. The calibration of the RVEDV and SV in PV loops outside the MRI subgroup (*n* = 50) is based on determination of the parallel conductance by the hypertonic saline method[18] and the slope factor alpha by combined Fick method and echo velocity time integral measurement. In comparison to MRI, especially the determination of SV by the latter methods seems more error prone. However, in contrast to the individual parameter Ees (Ees = Piso − Pes/SV) and Ea (Pes/SV), the SV is no longer part of the Ees/Ea ratio, because the equation will mathematically result in Ees/Ea = (Piso/Pes) − 1.[19,38] Similar to Tello et al.,[5] the SB method of PV-loop analysis was used without validation against the gold standard of multi-beat measurements. However, Bland–Altmann analysis of two different precapillary PH cohorts showed reasonable agreement between SB and multi-beat Ees/Ea when the ratio is <1.[6,26] In addition, despite the independent prognostic value of baseline RV-PA coupling in secondary PH, during the follow-up observation of our specific study population, the LV response or non-response to CRT therapy may have affected all-cause mortality[12] and RV-PA coupling efficiency. Furthermore, long-lasting PH may influence late RV-PA coupling capacity and survival.[39] Longer studies could provide clarification.

In addition, more data are needed to clarify the role of diastolic RV function in HFREF ± secondary PH. Increased early and end-diastolic filling pressures are not only the result of decreased RV relaxation and increased stiffness but may also be highly influenced by the diastolic and systolic LV-dysfunction (ventricular interaction) and by increasing pericardial constraint depending on biventricular dilatation and distensibility of the pericardium.

In conclusion, we demonstrate that RV SB Ees/Ea is closely associated with RV size and function and predicts overall survival of a HFREF cohort with secondary PH, even after key adjustments. The best cut-off for Ees/Ea to discriminate prognosis is 0.68, which corresponds highly significant to the non-invasive surrogate echo-parameters of RV-PA coupling such as TAPSE of 16 mm, FAC of 42%, and MRI-derived RVEF of 38% and SV/ESV of 0.59. Prognostically favourably coupled PH patients (Ees/Ea ≥ 0.68) were associated with a preserved RV size and function and a mid-term survival that was comparable to HFREF without PH. In contrast, haemodynamically uncoupled patients (Ees/Ea < 0.68) were regularly affiliated with dilated and systolic/diastolic dysfunctional RV, which were associated with a dramatic increase of short-term and medium-term all-cause mortality. Independent risk factors for unfavourable coupling were low LV-EF (<30%) and high pulsatile load (PA compliance <2.3 mL/mmHg). Haemodynamic RV-PA coupling closely correlates to non-invasive parameters of RV size, function, and prognosis. This transmission into parameters easily determined makes our findings attractive for a better clinical risk stratification and decision-making process for the timing of left ventricular assist devices and/or heart transplantation in patients with HFREF and secondary PH. However, further work is needed to elucidate the complex interaction of RV with pulmonary vascular afterload and/or LV/LA dysfunction, including comparisons of the different SB methods with multi-beat approaches for the analysis of intrinsic contractility and consecutive RV-PA coupling.

Conflict of interest

There is no conflict of interest.

Funding

Supporting information

Additional supporting information may be found online in the Supporting Information section at the end of the article.

Figure S1: A: Determination of RV end-systolic elastance (EA), PA-effective EA and RV-PA coupling by single-beat (SB) estimation.

Left: The maximal RV pressure (P_{max}) for an isovolumic (non-ejecting) beat (P_{iso}) at the existing end-diastolic volume (EDV) was estimated by fitting a fifth-order polynomial to the RV pressure curve, excluding all data points between the moments of maximal and minimal dP/dT and those after the time point when dP/dT increase above 10% of dP/dT_{min}.

Right: P_{iso} of isovolumic beats is drawn on RV pressure-volume (PV) curve. The ESPVR line is drawn from predicted $P_{iso} = P_{max}$ down and the tangent to the actual ejecting beat end systole (ESP, end-ejecting, however > dP/dT_{min}) and to the V_{25}. Ees is determined by P_{iso} - ESP/ stroke volume. V_{25} is the intercept of the ESPVR at an end-systolic pressure level of 25 mmHg. The Ea is the absolute slope of the PA EA line joining the RV ESP volume point to the point on the volume axis at the EDV, where SV represents the stroke volume. The ESV represents end-systolic volume. The RV-PA coupling efficiency is determined by the quotient of SB-Ees/SB-Ea. A PV loop area (PVA) was calculated as the sum of the potential energy (PE) and stroke work (SW), and the mechanical efficiency (ME) as the quotient SW/PVA.

Figure S2: Receiver operating characteristic (ROC) curve analysis of the pressure volume (PV) loop-derived Ees/Ea to discriminate survival from all-cause mortality in patients with secondary PH (PA mean ≥ 25 mmHg). (HFREF: heart failure with reduced ejection fraction, PH: pulmonary hypertension, PA: pulmonary arterial).

Figure S3: ROC analysis of PA compliance, LV-EF, and RVEDV for discriminating prognostically relevant RV-PA coupling, dichotomized at an Ees/Ea of 0.68.

(PA compliance, RVEDV, and LV-EF were evaluated together within one ROC model.

AUC: area under the curve, RVEDV: RV end-diastolic volume, LV-EF: left ventricular ejection fraction).

Figure S4: Representative PV-loops and SB analysis in HFREF patients without PH (No-PH) and PH stratified by an Ees/Ea of 0.68. (Ees: RV end-systolic elastance, Ea: arterial end-systolic elastance, PH: pulmonary hypertension, ESV_{25}: end-systolic volume at pressure of 25 mmHg).

Figure S5: Presentation of selected correlations between PV loop-derived Ees, Ea, and Ees/Ea with independent predictors of prognostically relevant coupling, defined by an Ees/Ea ratio ≥ 0.68 vs. < 0.68 in HFREF patients with secondary PH.

Figure S6: Association of PA compliance with LA pressure (PCWP) and the degree of MR.

Data S1. Supporting information.

Table S1: Bivariate correlation analysis (Spearman).

Table S2. Linear regression analysis of the relationship between hemodynamic PV loop-derived SB Ees/Ea and noninvasive displayable RV size and function in HFREF and secondary PH.

Table S3: Linear regression analysis of the relationship between hemodynamic PV loop-derived SB Ees and noninvasive displayable RV size and function in patients with HFREF and secondary PH.

Table S4: Linear regression analysis of the relationship between hemodynamic PV loop-derived SB Ees/Ea ratio and noninvasive displayable RV size and function in patients with HFREF without secondary PH.

References

1. Maughan WL, Shoukas AA, Sagawa K, Weisfeldt ML. Instantaneous pressure–volume relationship of the canine right ventricle. *Circ Res* 1979; **44**: 309–315.

2. Sanz J, Sánchez-Quintana D, Bossone E, Bogaard HJ, Naeije R. Anatomy, function, and dysfunction of the right ventricle: JACC state-of-the-art review. *J Am Coll Cardiol* 2019; **73**: 1463–1482.

3. Kass DA, Kelly RP. Ventriculo-arterial coupling: concepts, assumptions, and applications. *Ann Biomed Eng* United States 1992; **20**: 41–62.

4. Sagawa K, Maughan L, Suga H, Sunagawa K. *Cardiac Contraction and the Pressure–Volume Relationship*. New York: Oxford University Press; 1988.

5. Tello K, Dalmer A, Axmann J, Vanderpool R, Ghofrani HA, Naeije R, Roller F, Seeger W, Sommer N, Wilhelm J, Gall H, Richter MJ. Reserve of right ventricular-arterial coupling in the setting of chronic overload. *Circ Heart Fail* 2019; **12**: e005512.

6. Richter MJ, Peters D, Ghofrani HA, Naeije R, Roller F, Sommer N, Gall H, Grimminger F, Seeger W, Tello K. Evaluation and prognostic relevance of right ventricular-arterial coupling in pulmonary hypertension. *Am J Respir Crit Care Med* 2020; **201**: 116–119.

7. Pueschner A, Chattranukulchai P, Heitner JF, Shah DJ, Hayes B, Rehwald W, Parker MA, Kim HW, Judd RM, Kim RJ, Klem I. The prevalence, correlates, and impact on cardiac mortality of right ventricular dysfunction in nonischemic cardiomyopathy. *JACC Cardiovasc Imaging* 2017; **10**: 1225–1236.

8. Muslem R, Ong CS, Tomashitis B, Schultz J, Ramu B, Craig ML, Van Bakel AB, Gilotra NA, Sharma K, Hsu S, Whitman GJ, Leary PJ, Cogswell R, Lozonschi L, Houston BA, Zijlstra F, Caliskan K, Bogers AJJC, Tedford RJ. Pulmonary arterial elastance and INTERMACS-defined right heart failure following left ventricular assist device. *Circ Heart Fail* 2019; **12**: 1–11.

9. Rosenkranz S, Gibbs JSR, Wachter R, De Marco T, Vonk-Noordegraaf A, Vachiéry JL. Left ventricular heart failure and pulmonary hypertension. *Eur Heart J* 2016; **37**: 942–954.

10. Tedford RJ, Hassoun PM, Mathai SC, Girgis RE, Russell SD, Thiemann DR, Cingolani OH, Mudd JO, Borlaug BA, Redfield MM, Lederer DJ, Kass DA. Pulmonary capillary wedge pressure augments right ventricular pulsatile loading. *Circulation* 2012; **125**: 289–297.

11. Santamore WP, Dell'Italia LJ. Ventricular interdependence: significant left ventricular contributions to right ventricular systolic function. *Prog Cardiovasc Dis* United States 1998; **40**: 289–308.

12. Schmeisser A, Rauwolf T, Ghanem A, Groscheck T, Adolf D, Grothues F, Fischbach K, Kosiek O, Huth C, Kropf S, Lange S, Luani B, Smid J, Schäfer MH, Schreiber J, Tanev I, Wengler F, Yeritsyan NB, Steendijk P, Braun-Dullaeus RC. Right heart function interacts with left ventricular remodeling after CRT: a pressure volume loop study. *Int J Cardiol* Netherlands 2018; **268**: 156–161.

13. Zoghbi WA, Adams D, Bonow RO, Enriquez-Sarano M, Foster E, Grayburn PA, Hahn RT, Han Y, Hung J, Lang RM, Little SH, Shah DJ, Shernan S, Thavendiranathan P, Thomas JD, Weissman NJ. Recommendations for noninvasive evaluation of native valvular regurgitation: a report from the American Society of Echocardiography Developed in Collaboration with the Society for Cardiovascular Magnetic Resonance. *J Am Soc Echocardiogr* American Society of Echocardiography 2017; **30**: 303–371.

14. Lang RM, Badano LP, Victor MA, Afilalo J, Armstrong A, Ernande L, Flachskampf FA, Foster E, Goldstein SA, Kuznetsova T, Lancellotti P, Muraru D, Picard MH, Retzschel ER, Rudski L, Spencer KT, Tsang W, Voigt JU. Recommendations for cardiac chamber quantification by echocardiography in adults: an update from the American Society of Echocardiography and the European Association of Cardiovascular Imaging. *J Am Soc Echocardiogr* Elsevier Inc 2015; **28**: 1–39 e14.

15. Badagliacca R, Poscia R, Pezzuto B, Nocioni M, Mezzapesa M, Francone M, Giannetta E, Papa S, Gambardella C, Sciomer S, Volterrani M, Fedele F, Dario VC. Right ventricular remodeling in idiopathic pulmonary arterial hypertension: adaptive versus maladaptive morphology. *J Heart Lung Transplant* Elsevier 2015; **34**: 395–403.

16. Schmeisser A, Rauwolf T, Groscheck T, Kropf S, Luani B, Tanev I, Hansen M, Meißler S, Steendijk P, Braun-Dullaeus RC. Pressure–volume loop validation of TAPSE/PASP for right ventricular arterial coupling in heart failure with pulmonary hypertension. *Eur Heart J Cardiovasc Imaging* England 2021; **22**: 168–176.

17. Rosenkranz S, Diller G-P, Dumitrescu D, Ewert R, Ghofrani HA, Grünig E, Halank M, Held M, Kaemmerer H, Klose H, Kovacs G, Konstantinides S, Lang IM, Lange TJ, Leuchte H, Mayer E, Olschewski A, Olschewski H, Olsson KM, Opitz C, Schermuly RT, Seeger W, Wilkens H, Hoeper MM. Hemodynamic Definition of Pulmonary Hypertension: Commentary on the Proposed Change by the 6th World Symposium on Pulmonary Hypertension. *Dtsch Med Wochenschr* Germany 2019; **144**: 1367–1372.

18. Steendijk P, Staal E, Jukema JW, Baan J. Hypertonic saline method accurately determines parallel conductance for dual-field conductance catheter. *Am J Physiol Heart Circ Physiol* 2001; **281**: 755–763.

19. Brimioulle S, Wauthy P, Ewalenko P, Rondelet B, Vermeulen F, Kerbaul F, Naeije R. Single-beat estimation of right ventricular end-systolic pressure–volume relationship. *Am J Physiol Heart Circ Physiol* 2003; **284**: 1625–1630.

20. Ten Brinke EA, Klautz RJ, Verwey HF, Van Der Wall EE, Dion RA, Steendijk P. Single-beat estimation of the left ventricular end-systolic pressure–volume relationship in patients with heart failure. *Acta Physiol* 2010; **198**: 37–46.

21. Ten Brinke EA, Burkhoff D, Klautz RJ, Tschöpe C, Schalij MJ, Bax JJ, Van Der Wall EE, Dion RA, Steendijk P. Single-beat estimation of the left ventricularend-diastolic pressure–volume relationship in patients with heart failure. *Heart* 2010; **96**: 213–219.

22. Steendijk P. Right ventricular function and failure: methods, models, and mechanisms. *Crit Care Med* United States 2004: 1087–1089.

23. Dini FL, Conti U, Fontanive P, Andreini D, Banti S, Braccini L, De Tommasi SM. Right ventricular dysfunction is a major predictor of outcome in patients with moderate to severe mitral regurgitation and left ventricular dysfunction. *Am Heart J* United States 2007; **154**: 172–179.

24. Anavekar NS, Skali H, Bourgoun M, Ghali JK, Kober L, Maggioni AP, McMurray JJV, Velazquez E, Califf R, Pfeffer MA, Solomon SD. Usefulness of right ventricular fractional area change to predict death, heart failure, and stroke following myocardial infarction (from the VALIANT ECHO Study). *Am J Cardiol* United States 2008; **101**: 607–612.

25. Axell RG, Messer SJ, White PA, McCabe C, Priest A, Statopoulou T, Drozdzynska M, Viscasillas J, Hinchy EC, Hampton-Till J, Alibhai HI, Morrell N, Pepke-Zaba J, Large SR, Hoole SP. Ventriculo-arterial coupling detects occult RV dysfunction in chronic thromboembolic pulmonary vascular disease. *Physiol Rep* 2017; **5**: 1–13.

26. Hsu S, Simpson CE, Houston BA, Wand A, Sato T, Kolb TM, Mathai SC, Kass DA, Hassoun PM, Damico RL, Tedford RJ. Multi-beat right ventricular-arterial coupling predicts clinical worsening in pulmonary arterial hypertension. *J Am Heart Assoc* 2020; **9**: e016031.

27. van de Veerdonk MC, Marcus JT, Westerhof N, de Man FS, Boonstra A, Heymans MW, Bogaard H-J, Noordegraaf AV. Signs of right ventricular deterioration in clinically stable patients with pulmonary arterial hypertension. *Chest* United States 2015; **147**: 1063–1071.

28. Dupont M, Mullens W, Skouri HN, Abrahams Z, Wu Y, Taylor DO, Starling RC, Tang WHW. Prognostic role of pulmonary arterial capacitance in advanced heart failure. *Circ Heart Fail* 2012; **5**: 778–785.

29. Aquaro GD, Negri F, De Luca A, Todiere G, Bianco F, Barison A, Camastra G, Monti L, Dellegrottaglie S, Moro C, Lanzillo C, Scatteia A, Di Roma M, Pontone G, Perazzolo Marra M, Di Bella G, Donato R, Grigoratos C, Emdin M, Sinagra G. Role of right ventricular involvement in acute myocarditis, assessed by cardiac magnetic resonance. *Int J Cardiol* Netherlands 2018; **271**: 359–365.

30. Ondrus T, Kanovsky J, Novotny T, Andrsova I, Spinar J, Kala P. Right ventricular myocardial infarction: From pathophysiology to prognosis. *Exp Clin Cardiol* 2013; **18**: 27–30.

31. Ghio S, Gavazzi A, Campana C, Inserra C, Klersy C, Sebastiani R, Arbustini E, Recusani F, Tavazzi L. Independent and additive prognostic value of right ventricular systolic function and pulmonary artery pressure in patients with chronic heart failure. *J Am Coll Cardiol* United States 2001; **37**: 183–188.

32. Rogers JG, Pagani FD, Tatooles AJ, Bhat G, Slaughter MS, Birks EJ, Boyce SW, Najjar SS, Jeevanandam V, Anderson AS, Gregoric ID, Mallidi H, Leadley K, Aaronson KD, Frazier OH, Milano CA. Intrapericardial left ventricular assist device for advanced heart failure. *N Engl J Med* United States 2017; **376**: 451–460.

33. Reichenbach A, Al-Hiti H, Malek I, Pirk J, Goncalvesova E, Kautzner J, Melenovsky V. The effects of phosphodiesterase 5 inhibition on hemodynamics, functional status and survival in advanced heart failure and pulmonary hypertension: a case-control study. *Int J Cardiol* Elsevier Ireland Ltd 2013; **168**: 60–65.

34. Gulati G, Grandin EW, Kennedy K, Cabezas F, DeNofrio DD, Kociol R, Rame JE, Pagani FD, Kirklin JK, Kormos RL, Teuteberg J, Kiernan M. Preimplant phosphodiesterase-5 inhibitor use is associated with higher rates of severe early right heart failure after left ventricular assist device implantation an INTERMACS analysis. *Circ Heart Fail* 2019; **12**: 1–10.

35. Borlaug BA, Melenovsky V, Marhin T, Fitzgerald P, Kass DA. Sildenafil inhibits β-adrenergic-stimulated cardiac contractility in humans. *Circulation* 2005; **112**: 2642–2649.

36. Vachiéry J-L, Tedford RJ, Rosenkranz S, Palazzini M, Lang I, Guazzi M, Coghlan G, Chazova I, De Marco T. Pulmonary hypertension due to left heart disease. *Eur Respir J* 2019; **53**: 1801897.

37. Monzo L, Reichenbach A, Al-Hiti H, Borlaug BA, Havlenova T, Solar N, Tupy M, Ters J, Kautzner J, Melenovsky V. Acute unloading effects of sildenafil enhance right ventricular–pulmonary

artery coupling in heart failure. *J Card Fail* Elsevier Inc. 2020; **27**: 224–232.

38. Vanderpool RR, Pinsky MR, Naeije R, Deible C, Kosaraju V, Bunner C, Mathier MA, Lacomis J, Champion HC, Simon MA. RV-pulmonary arterial coupling

predicts outcome in patients referred for pulmonary hypertension. *Heart* 2015; **101**: 37–43.

39. Wright SP, Groves L, Vishram-Nielsen JKK, Karvasarski E, Valle FH, Alba AC, Mak S. Elevated pulmonary arterial

elastance and right ventricular uncoupling are associated with greater mortality in advanced heart failure. *J Hear lung Transplant Off Publ Int Soc Hear Transplant* United States 2020; **39**: 657–665.